Electronic Supplementary Material (ESI) for Inorganic Chemistry Frontiers.

Supporting Information

Preparation of Inorganic-Framework Molecular Imprinted TiO_2/SiO_2 Nanofibers by One-Step Electrospinning and its Highly Selective Photodegradation

Jingyao Li,[a] Yanhua Song,[a] Fangke Wang,[a] Xiaozhen Zhang,[a] Haiyuan Zhu,[a] and Haifeng Zou*[a]

[a] College of Chemistry, Jilin University, Qianjin Street 2699, Changchun 130012, China.

Corresponding Author:

*E-mail: haifengzou0431@sohu.com

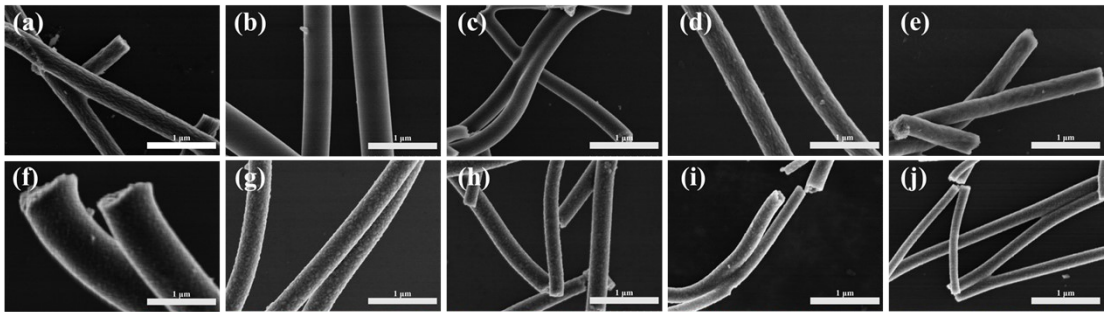

Figure S1. SEM images of (a)-(e) STN-STM0.1 and (f)-(j) TN-TM0.1 products

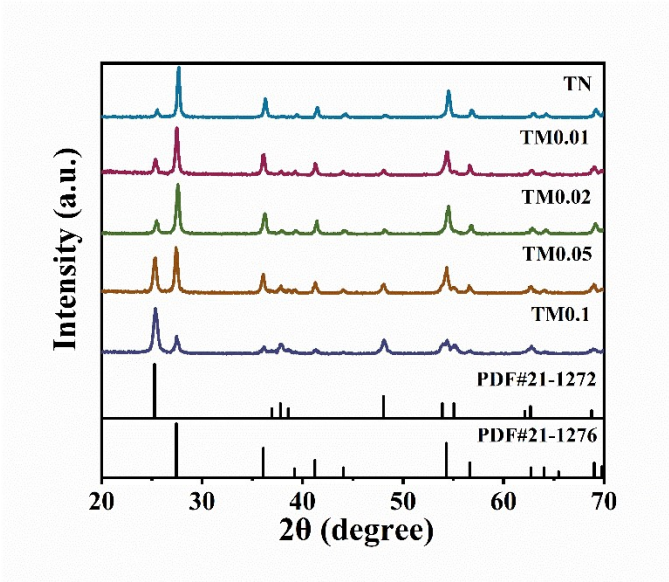

Figure S2. XRD patterns of samples TN-TM0.1 and corresponding standard data of anatase (PDF#21-1272) and rutile (PDF#21-1276)

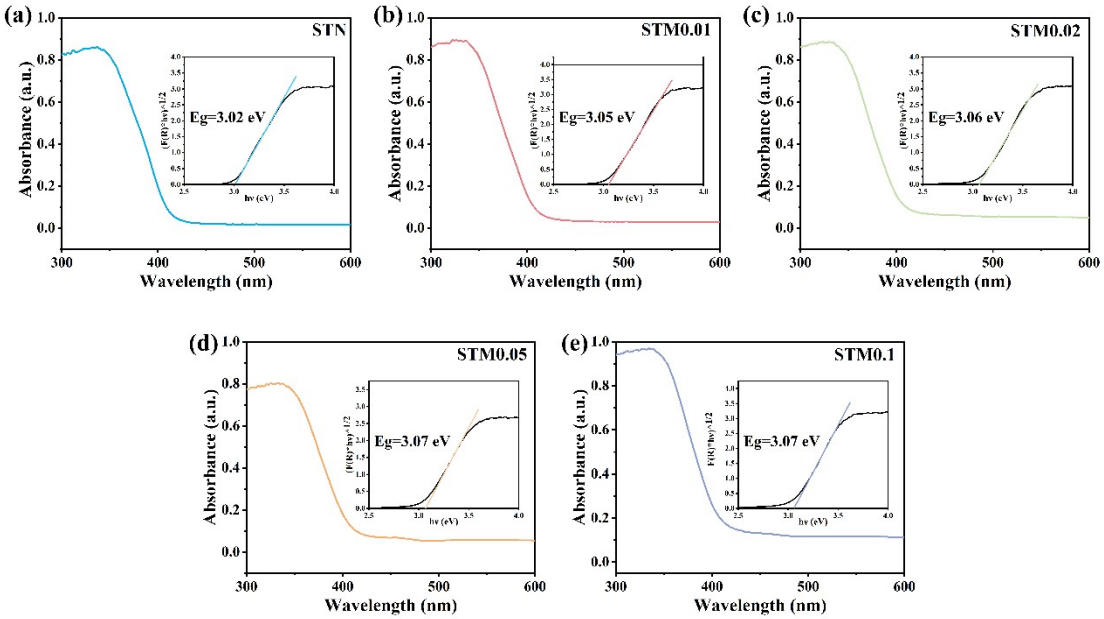

Figure S3. UV-vis diffuse reflectance spectra and corresponding band-gap energy spectra (inset) of STN (a), STM0.01 (b), STM0.02 (c), STM0.05 (d), STM0.1 (e) products

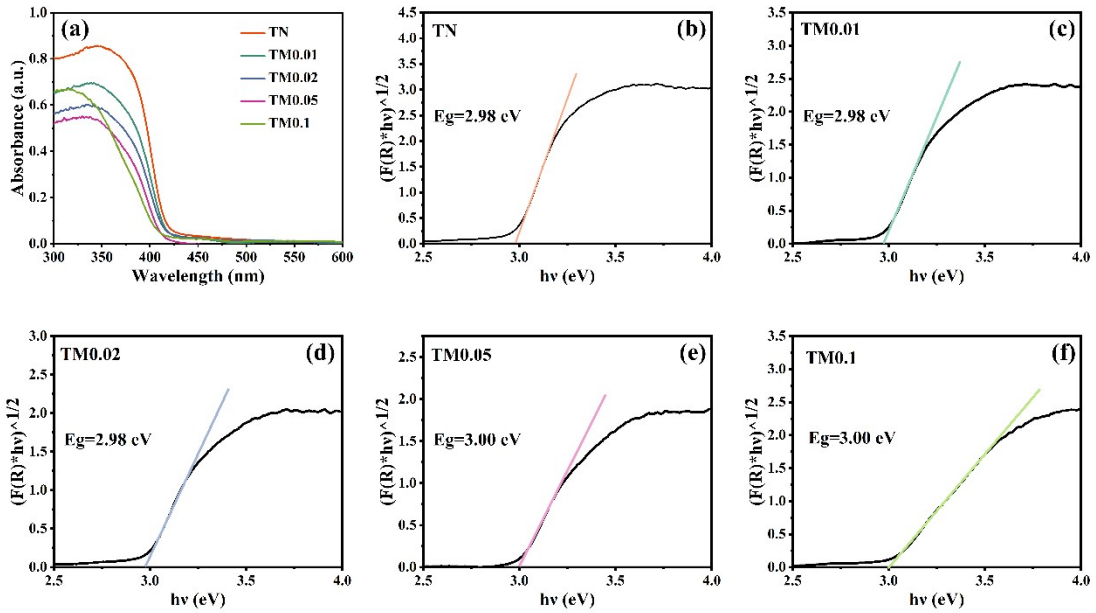

Figure S4. (a) UV-vis spectra and (b-f) $(F(R)*hv)^{1/2}$-hv curves of TN, TM0.01, TM0.02, TM0.05 and TM0.1

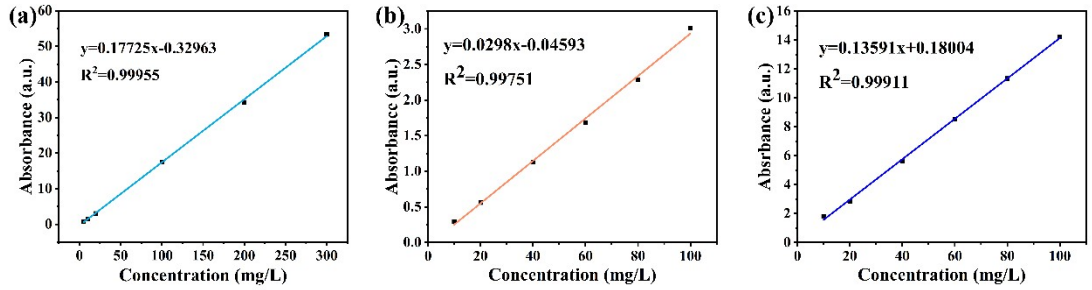

Figure S5. The standard curves of RhB (a), MO (b), MB (c)

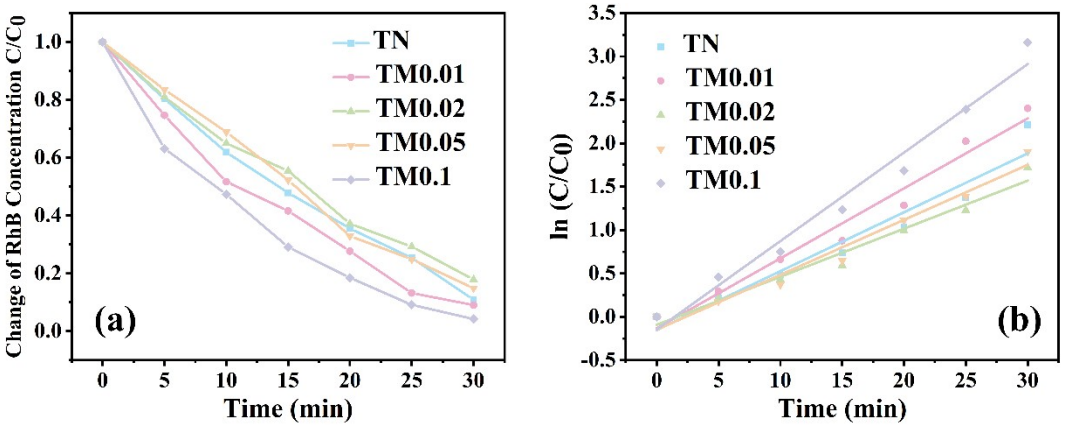

Figure S6. (a) Photodegradation efficiency curves of RhB by TN, TM0.01, TM0.02, TM0.05 and TM0.1 (b) Corresponding kinetic linear simulation curves of RhB photodegradation

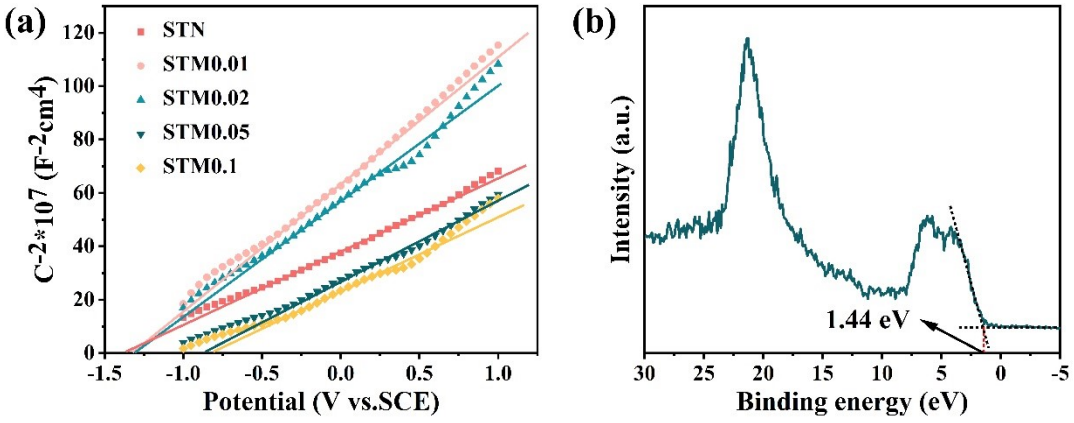

Figure S7. (a) Mott-Schottky curves of as-prepared photocatalysts and (b) VB

spectrum of STM0.05

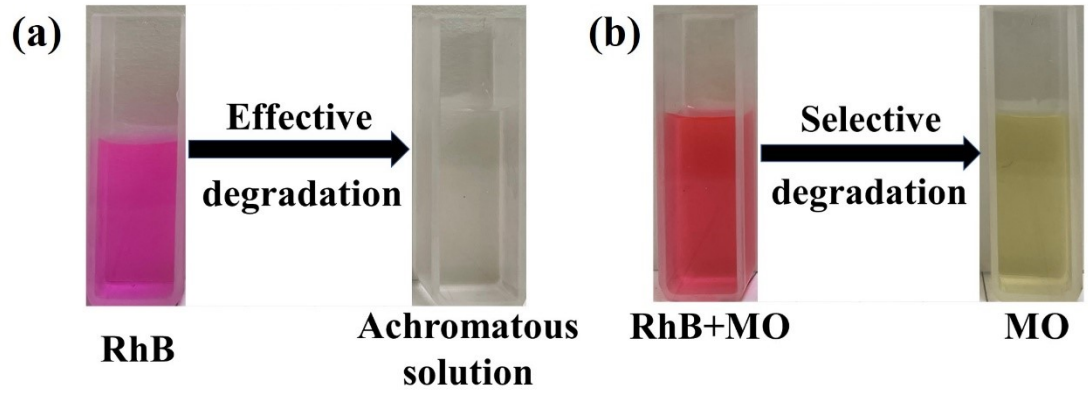

Figure S8. Digital images of solutions of (a) RhB and (b) RhB and MO mixture before and after photodegradation

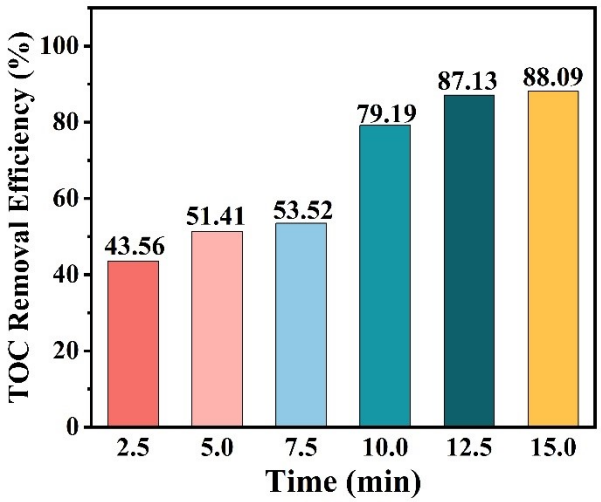

Figure S9. TOC removal efficiency of RhB by STM0.05 at different time.

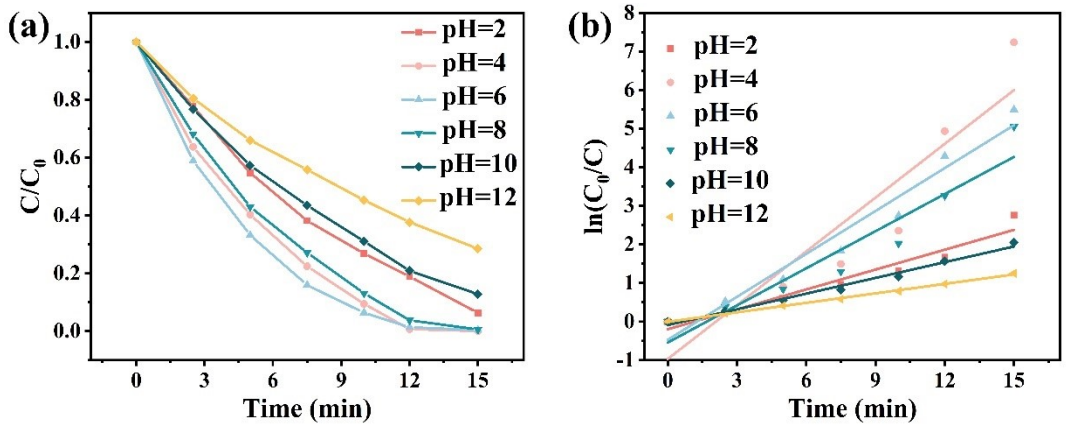

Figure S10. (a) Photodegradation curves of RhB by STM0.05 at different solution pH and (b) corresponding pseudo-first-order kinetics fitting curves.

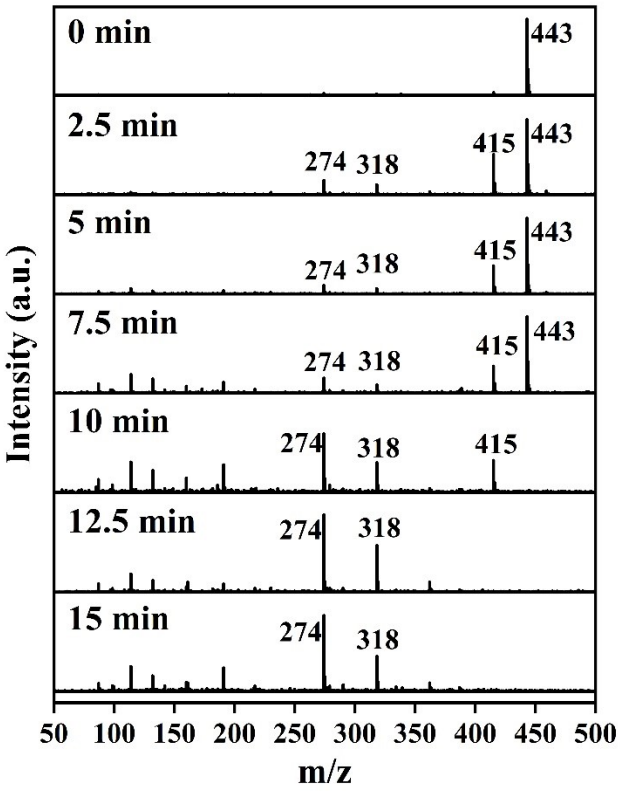

Figure S11. Mass spectra of degradation products of RhB by STM0.05.

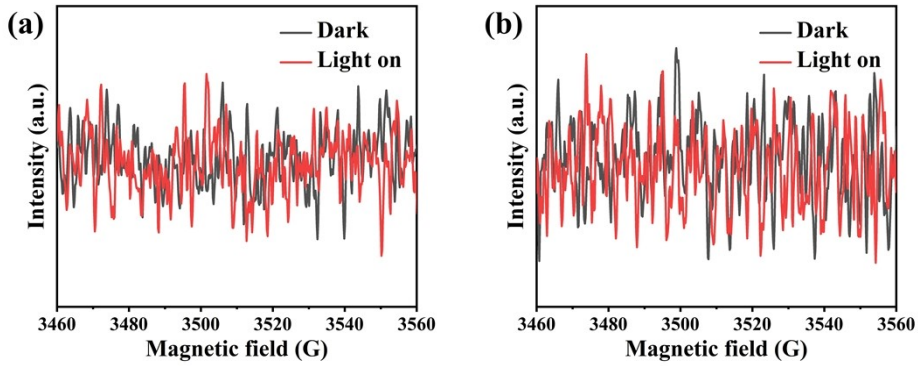

Figure S12. EPR spectra of STM0.05 in RhB degradation of (a) DMPO-$\cdot O_2^-$ and (b) DMPO-·OH.

Table S1. The calculated crystal sizes and phase compositions of the prepared samples

Samples	Grain Size (nm)	Phase Composition (%)	
		Anatase	Rutile
STN	15.06	71.41	28.59
STM0.01	12.43	89.13	10.87
STM0.02	12.25	90.12	9.88
STM0.05	11.19	100	0
STM0.1	10.20	100	0
TN	26.52	9.53	90.47
TM0.01	24.17	17.26	82.74
TM0.02	24.02	18.81	81.19
TM0.05	23.58	42.24	57.76
TM0.1	19.54	74.92	25.08

Table S2. Kinetic Parameters Calculated from the Pseudo-First-Order Kinetics and Pseudo-Second-Order Kinetics

Kinetics Model	Parameters	STN	STM0.01	STM0.02	STM0.05	STM0.1
Pseudo-first-order kinetics	R^2	0.90745	0.91906	0.08825	0.80074	0.03032
	K_1	0.00873	0.00941	0.00284	0.02206	0.00467
	$Q_{e,cal}$	1.54467	4.357332	1.670812	5.141783	5.652681
Pseudo-second-order kinetics	R^2	0.99964	0.99696	0.99836	0.99936	0.99482
	K_2	0.107	0.0289	0.082	0.056	0.073
	$Q_{e,cal}$	4.57	8.352	9.022	9.918	9.281
□	h	3.106	3.14	8.538	6.589	13.446

Table S3. Zeta potential values of as-prepared samples

Samples	**Zeta potential (mV)**
STN	-17.92
STM0.01	-27.97
STM0.02	-35.00
STM0.05	-39.70
STM0.1	-37.52

Table S4. Comparison of RhB degradation by various photocatalysts

Photocatalysts	Dosage (g/L)	RhB concentration (mg/L)	Degradation efficiency (%)	Reaction time (min)	Reference
STM0.05	0.33	15	100	15	This work
MIL-88A(Fe)-GO-H_2O_2	0.4	10	100	80	[1]
g-C_3N_4/WO_3/NCDs	0.4	10	80	60	[2]
V_2O_5/g-C_3N_4	0.5	10	95.5	60	[3]
g-C_3N_4/CdO	1.5	10	96	120	[4]
Bi_2O_3/g-C_3N_4	0.25	10	83	180	[5]

References

[1] N. Liu, W. Huang, X. Zhang, L. Tang, L. Wang, Y. Wang, M. Wu, Ultrathin graphene oxide encapsulated in uniform MIL-88A(Fe) for enhanced visible light-driven photodegradation of RhB, Applied Catalysis B: Environmental 221 (2018) 119-128. https://doi.org/10.1016/j.apcatb.2017.09.020.

[2] J. Jia, C. Jiang, X. Zhang, P. Li, J. Xiong, Z. Zhang, T. Wu, Y. Wang, Urea-modified carbon quantum dots as electron mediator decorated g-C3N4/WO3 with enhanced visible-light photocatalytic activity and mechanism insight, Applied Surface Science 495 (2019) 143524-143534. https://doi.org/10.1016/j.apsusc.2019.07.266.

[3] Y. Hong, Y. Jiang, C. Li, W. Fan, X. Yan, M. Yan, W. Shi, In-situ synthesis of direct solid-state Z-scheme V2O5/g-C3N4 heterojunctions with enhanced visible light efficiency in photocatalytic degradation of pollutants, Applied Catalysis B: Environmental 180 (2016) 663-673. https://doi.org/10.1016/j.apcatb.2015.06.057.

[4] T.D. Munusamy, C.S. Yee, M.M.R. Khan, Construction of hybrid g-C3N4/CdO nanocomposite with improved photodegradation activity of RhB dye under visible light irradiation, Advanced Powder Technology 31(7) (2020) 2921-2931.

https://doi.org/10.1016/j.apt.2020.05.017.

[5] M. Ben Abdelaziz, B. Chouchene, L. Balan, T. Gries, G. Medjahdi, H. Ezzaouia, R. Schneider, One pot synthesis of bismuth oxide/graphitic carbon nitride composites with high photocatalytic activity, Molecular Catalysis 463 (2019) 110-118. https://doi.org/10.1016/j.mcat.2018.12.004.